Legros, Alexandre; Nissi, Janita; Laakso, Ilkka; Duprez, Joan; Kavet, Robert; Modolo, Julien

Thresholds and mechanisms of human magnetophosphene perception induced by low frequency sinusoidal magnetic fields

Published in:
Brain Stimulation

DOI:
10.1016/j.brs.2024.05.004

Published: 01/05/2024

Document Version
Publisher's PDF, also known as Version of record

Brain Stimulation 17 (2024) 668–675

Contents lists available at ScienceDirect

Brain Stimulation

journal homepage: www.journals.elsevier.com/brain-stimulation

Thresholds and mechanisms of human magnetophosphene perception induced by low frequency sinusoidal magnetic fields

Alexandre Legros [a,b,c,d,*], Janita Nissi [e], Ilkka Laakso [e], Joan Duprez [g], Robert Kavet [f], Julien Modolo [a,g]

[a] Human Threshold Research Group, Lawson Health Research Institute, London, ON, Canada
[b] Departments of Medical Biophysics and Medical Imaging Western University, London, ON, Canada
[c] School of Kinesiology, Western University, London, ON, Canada
[d] EuroMov Digital Health in Motion, University of Montpellier and IMT Mines Ales, Montpellier, France
[e] Department of Electrical Engineering and Automation, Aalto University, Espoo, Finland
[f] Kavet Consulting LLC, Oakland, CA, USA
[g] Univ Rennes, INSERM, LTSI – U1099, F-35000, France

ARTICLE INFO

Keywords:
Extremely low-frequency magnetic fields
Power-line frequency magnetic fields
Magnetophosphenes
Human
Electroencephalography

ABSTRACT

Background: Virtually everyone is exposed to power-frequency MF (50/60 Hz), inducing in our body electric fields and currents, potentially modulating brain function. MF-induced electric fields within the central nervous system can generate flickering visual perceptions (*magnetophosphenes*), which form the basis of international MF exposure guidelines and recommendations protecting workers and the general public. However, magnetophosphene perception thresholds were estimated 40 years ago in a small, unreplicated study with significant uncertainties and leaving open the question of the involved interaction site.

Methods: We used a stimulation modality termed transcranial alternating magnetic stimulation (tAMS), delivering *in situ* sinusoidal electric fields comparable to transcranial alternating current stimulation (tACS). Magnetophosphene perception was quantified in 81 volunteers exposed to MF (eye or occipital exposure) between 0 and 50 mT at frequencies of 20, 50, 60 and 100 Hz.

Results: Reliable magnetophosphene perception was induced with tAMS without any scalp sensation, a major advantage as compared to tACS. Frequency-dependent thresholds were quantified using binary logistic regressions hence allowing to establish condition dependent probabilities of perception. Results support an interaction between induced current density and retinal rod cells.

Conclusion: Beyond fundamental and immediate implications for international safety guidelines, and for identifying the interaction site underlying phosphene perception (ubiquitous in tACS experiments), our results support exploring the potential of tAMS for the differential diagnosis of retinal disorders and neuromodulation therapy.

1. Introduction

In 1896, Jacques-Arsène d'Arsonval (a French physician) experienced a *magnetophosphene* from a 42-Hz magnetic field (MF) of unreported magnitude [1]. Subsequent studies in humans confirmed electro- and magneto-phosphene phenomena with maximal sensitivity at about 20 Hz[2–8], with some examining effect details (e.g., ambient lighting effects) [2,3] and their interaction site using various laboratory preparations (e.g., frog retina) [4,5–7]. The perception of phosphenes is also common in transcranial alternating current stimulation (tACS) experiments, which is a key issue since this can compromise blinding to the stimulation condition, in addition to be a confounding factor when attempting as disentangling the effects of tACS on brain circuits. This has motivated studies quantifying precisely the perception of (electro-) phosphenes as a consequence of tACS in various montages in humans [8]. Since phosphene perception is ubiquitous in tACS experiments, our identification of the underlying interaction site has significant implications for this field.

Electro and magneto-phosphenes are the most reliable indicators of the central nervous system's (CNS) response to MF, and they have

* Corresponding author. Human Threshold Research Group, Lawson Health Research Institute, 268 Grosvenor Street, London, ON, N6A 4V2, Canada.
E-mail address: alegros@lawsonimaging.ca (A. Legros).

https://doi.org/10.1016/j.brs.2024.05.004
Received 22 December 2023; Received in revised form 7 May 2024; Accepted 7 May 2024
Available online 11 May 2024

accordingly been adopted by international bodies as a basis for low-frequency (~<400–760 Hz) MF exposure limits [9,10]. The perception of magnetophosphenes is indeed the most reliable, reproducible biological (and not adverse *per se*) effect occurring in humans as a consequence of ELF MF with the lowest possible MF flux density. Therefore, magnetophosphene perception is at the core of the international guidelines and recommendations that protect the general public and workers worldwide, while the underlying assumption that adverse effects would occur at higher MF flux densities than this physiological, non-adverse reproducible biological response.

Although recent studies investigated the threshold for phosphene perception and associated frequency response [11–14], the threshold for magnetophosphenes at domestic frequencies (i.e. 50 and 60 Hz) is only extrapolated since no experimental data at this frequency in humans are available yet, contributing to the remaining uncertainties regarding magnetophosphene perception threshold in humans at power-frequency [15,16]. Furthermore, it has been and still is argued that magnetophosphene perception could occur from direct visual cortex activation [11,17], despite dosimetric inconsistencies [18,19], leaving the question still unresolved.

Here, to establish a sound basis for further study of magnetophosphenes, their interaction site and relationship with the visual system, we went beyond the state-of-the-art by addressing two major unresolved issues, using a stimulation modality that we term transcranial alternating magnetic stimulation (tAMS). First, while previous studies had not exposed subjects to frequencies greater than 45 Hz, leaving extrapolations as the only way to evaluate response characteristics for power frequency environmental MFs (60 Hz in North America; 50 Hz in Europe, generated by power lines, sources within residences etc.), here we explicitly tested power frequency MF for magnetophosphene perception. Second, with respect to modality, Kanai et al. reported that exposures of the occipital cortex to tACS produced phosphenes, suggesting a pathway for current to spread from the occiput to the retina [11], despite conflicting results from a later dosimetry study which suggested direct retinal stimulation by the MF [19]. Here, we included three distinct modalities to either confirm or refute these previous findings, along with dosimetric analyses using an anatomically accurate 3D head model to differentiate induced electric field patterns for each modality. Let us mention that tAMS should not been confused with TMS, since tAMS is based on sinusoidal, low-magnitude MFs (as opposed to pulsed, high-magnitude MFs in the case of TMS).

Overall, we establish magnetophosphene thresholds in humans exposed to MFs up to 50 mT between 20 and 100 Hz using tAMS, while confirming the site of interaction leading to magnetophosphene perception (e.g., retina or visual cortex). Providing precise and reliable thresholds for magnetophosphene perception in humans at power-frequencies and shedding light on their site of generation will be instrumental in the current process of re-evaluating international Standards and Guidelines protecting the public and workers from potential adverse effects of ELF exposures. Furthermore, those results support the use of tAMS to achieve neuromodulatory effects comparable to tACS in humans, while providing notable practical advantages.

2. Materials and methods

Eighty-one (81) healthy volunteers were recruited and tested in the Human Threshold Research Facility at St. Joseph's Hospital in London, Ontario, Canada. Volunteers with eye or retinal problems, history of claustrophobia, head injury, neurological and cardiovascular diseases were excluded. Furthermore, volunteers having permanent metal devices above the neck or stimulators (i.e., implanted neural stimulator, implanted cardiac pacemaker, auto-defibrillator, cochlear implants, and insulin pump) were ineligible. Finally, participants were instructed to refrain from exercise and alcohol, caffeine, or nicotine for 24 h preceding their exposure sessions. Study subjects were distributed randomly into four (4) groups: n = 20 at 20, 60 and 100 Hz; n = 21 at 50 Hz.

2.1. Magnetic field exposure systems

The systems consisted of an MRI gradient amplifier powering two systems of coils: one for local exposures (RET and OCC) and one for GLO. The system generates flux densities of up to 80 mT_{rms} at frequencies between 20 and 100 Hz. Here, the maximum flux density used was 50 mT_{rms}.

2.2. The MRI gradient amplifiers

Three MTS 0106475 MRI gradient amplifiers (MTS Automation 433 Caredean Dr. Horsham PA, USA – now owned by Performance Control Inc. 151 Domorah Drive, Montgomeryville, PA 18936 USA) were used to power the coil systems. These MTS amplifiers have an output impedance of 0.15 Ohms and are rated for 208 V, 3 phases, 80 A inputs with an output of 345 V, 200 A_{rms} for durations of over 300 s. The maximum current output is limited to ~180 A_{rms} when a rise time limitation is imposed for frequencies between 20 and 100 Hz.

2.3. Exposure coil systems

RET and OCC systems each consisted of a single coil, (the "local exposure coil"). The second coil system, the "global head exposure system," was designed for exposure of the entire head. Both systems were classified "Medical Grade" by the Canadian Standard Association (CSA: QFE-12061-3 and QFE-12061-6 respectively), which is the regulatory agency for hospital-based equipment in Canada.

Both the GLO and local systems (RET and OCC) consisted of hollow copper wire, with outer dimensions of 6.35 and 5 mm, respectively, and inner circular diameters of 3.5 and 3 mm, respectively. Coolant circulated within the windings to partially dissipate the heat generated by the currents. Cold water at ≈ 10 °C circulating through the copper tubing at a flow rate of 0.8 L/min drained ~1800 W of excess heating. To minimize coil vibration, the copper tubing was impregnated with thermal epoxy. This "wet winding technique" was outsourced to Stimple & Ward Co. (Pittsburgh Pa., USA). The resulting coils were therefore a compact solid circular assembly of wire with no air gap between windings. The coils were then mounted and bonded to custom-made PVC frames including brass ports designed and fabricated to facilitate plumbing and the coils' access to electrical connections.

2.4. Local retinal and occipital exposure

RET and OCC exposures were delivered using the same local exposure system (Supp. Fig. 3, Panels A and C), consisting of a single 176-turn coil (11 turns of 16 layers over a thickness of 6.2 cm, with an inner diameter of 6 cm, and an outer diameter of 22 cm). For RET, the center of the coil was tangential to the external side of the eye, centered on the eyeball (Fig. 3, Panel A), whereas for OCC, the center of the coil was centered on the occiput, at the back of the head (Supp. Fig. 3, Panel C).

2.5. Global head exposure

The GLO system consisted of a pair of 99-turn coils of 21.425 cm average radius each (11 layers of 9 turns each, 35.6 cm of inner diameter and 50.1 cm of outer diameter). The two coils were assembled into a Helmholtz-like configuration, spaced 20.6 cm from center to center (Supp. Fig. 3, Middle Panel). The coil array weighed about 80 kg and was secured by a motorized platform above the participant's shoulders. This platform, designed in-house, was fabricated from non-ferrous materials, and outsourced to the Engineering Machine Shop at Western University (London, ON, Canada) for assembly and certification. For additional security, we added a safety lock system supporting twice the coils' weight. The system enabled vertical positioning of participants

without any contact with the coil system.

2.6. LabVIEW-driven MRI gradient amplifiers

The currents flowing in the coil systems were controlled, using of a LabVIEW$_{TM}$ script (LabVIEW 2014 version 14.0.1 (32 bit), National Instrument, Austin, Texas) feeding a 16-bit National Instruments A/D Card output channel (National Instruments, Austin, TX), driving 3 MRI gradient amplifiers (one for each coil - MTS Automation Model No. 0105870, Horsham, PA, USA). These amplifiers operated in a controlled current mode, which is ideal for driving inductive loads by matching the coil current to the input signal voltage. This had enabled the generation of high-fidelity complex waveforms. Both the measured MF and button press data were recorded using the LabVIEW$_{TM}$ script.

2.7. Experimental procedure

For each frequency-modality (4x3 combinations), each subject was exposed to 11 MF levels (0–50 mT with 5 mT increments) presented in random order, as assigned by the LabVIEW program, following a double-blinded protocol. Subjects were seated and tested after a 5-min adaptation period to the darkness, which maintained through the exposure session. A volunteer was exposed to 5 *Trials* of each MF field level, each 5-s long separated by a 5-sec rest period. During each *Trial*, a subject had the opportunity to register perception of the field by pressing a button on a pad attached to the right armrest adjacent to the right index finger. Thus, each *Trial* resulted in a binary (yes/no or 1/0) response. This protocol was approved by the Health Sciences Research Ethics Board of Western University (HSREB #18882).

2.8. Exposure-response analysis

The MF at all frequencies (f) is sinusoidal expressed as:

$$B = B_0 \sin(2\pi ft)$$

With B_0 = field amplitude (mT)

The convention in this paper is to express the *RMS* quantities, as exposure guidelines and standards typically express exposure and dose limits in these terms.

The key dosimetric parameters are the current density (J) and the electric field (E-field) induced in brain or retina. This quantity is directly proportional to dB/dt, such that,

$$(dB/dt)_{RMS} = 2\pi f B_{RMS}$$

The use of dB/dt as a metric has several key advantages. First, since the induced electric field (per Maxwell-Faraday's law) is proportional to dB/dt, this provides us with a metric that takes frequency into account (since the derivative of a sine is a cosine with frequency as a multiplicative factor). Second, this facilitates comparisons with previous literature, where dB/dt has been widely used as a metric (as done in Supplementary Fig. 2).

For each frequency, the 1/0 binary responses were entered into a mixed logistic regression model with predictor (or independent) variables (1) the dB/dt (with RMS implied) and (2) the coil position (RET, OCC or GLO), and a random intercept for each participant. With 1's or 0's as dependent variables the model was formulated as:

$$P_{Response} = 1 / (1 + \exp(-(a + b*[dB/dt]))) \quad (1)$$

The coefficients, b permits an estimate of the response odds ratio per increment of dB/dt.

Mixed logistic regression modelling was performed using R (v. 4.3.2); implemented with the lme4 package [20–22]. The glmer function of the lme4 package was used for the model and each coil position was used as the reference condition to calculate the estimates using the following formula:

Model = glmer(dependent variable ~ Coil position + dBdt + (1|Subject), family = binomial, data = data, glmerControl (optimizer = "bobyqa"))

In order to differentiate the effect of dB/dt between the different coil positions, a similar model was fitted separately for each coil position, with the 1/0 binary response as dependent variable, and dB/dt as a fixed effect, and a random intercept for each participant. Before fitting these coil-specific models, we verified for each frequency-specific full model (containing both coil position and dB/dt as fixed effects) that a coil position x dB/dt interaction was significantly present, which was the case for all frequencies (all interaction pvalues <0.01).

The glmer function calculates significance of the estimates was calculated by asymptotic Wald tests. Finally, a Bonferroni correction was applied, resulting a threshold for significance of 0.05/12 (12 being the number of models fitted), i.e. a threshold of $p = 0.0041$.

2.9. Dosimetric analysis

The methods were described previously in Nissi and Laakso [23]. Briefly, magnetically induced electric field and current density were calculated with an algorithm based on the finite element method used in Hirata & Laakso [19] inside anatomical head models created from magnetic resonance images [24]. Global and local coils were modeled with thin wire approximations and were positioned as in the experiments. Comparison of the measured and modeled magnetic fields confirmed the validity of the coil models (Supp. Fig. 3).

Fourteen head models were used with a resolution of 0.5 mm and tissue conductivities shown in Table 3. Those head models were the same than those used in Nissi and Laakso [25] in order to enable comparisons of their induced current density values to those of the present study. The tissues were assumed homogeneous and isotropic with respect to conductivity. The models for the eyes included separate tissues for the sclera, cornea, retina, vitreous humor, lens, and optic nerve. The retina was modeled as a layer with a constant thickness of 0.5 mm. The 99th percentile value of the radial current density was calculated on the retinal surface within 90° and between 90° and 135° from the posterior pole of the eye as described in Nissi and Laakso [23]. Radial current densities (J_n) were first determined separately for all the models with means and standard deviations calculated for the sample. The radial current density is reported instead of the electric field, as it is continuous over the retina, and is thus unaffected by the retinal conductivity value [23], which is still uncertain. Due to the thinness of the retina, the radial electric field can be estimated by dividing the reported radial current density values with the retinal conductivity.

3. Results

The results broken out by each frequency-exposure modality combination are shown as regression curves in Fig. 1. For these same combinations, Table 1 shows the regressed coefficient values; their respective p-values; odds ratios (ORs) per unit increment of dB/dt, with their respective 95 % CIs; and Conditional r-squared, which reports the percentage of variance accounted for by the model.

Table 1 indicates that for both GLO and RET exposure modalities, the field coefficients dB/dt are all statistically significant, indicating ORs that exclude the null hypothesis. For GLO and RET, the Conditional r-squared indicates that the model predicts relatively high values of explained variance of between 24 % and 70 %. For OCC, no magnetophosphene perception was evoked significantly at 20 and 50 Hz, but the dB/dt coefficients were statistically significant at 60 and 100 Hz, with the full model accounting for levels of 37 % and 23 % variance explained, respectively.

Finally, to the question "can you describe what you perceived when you pressed the button? Did it have a specific color?", all subjects but one out of 81 reported "white" (colorless) phosphenes. Both

Table 1
Coefficients from mixed model logistic regressions (Eq. (1)) by frequency and exposure modality, shown with their respective *p*-values, response odds ratios (*OR*) (with 95 % *CIs*) per increment of *dB/dt* (T/s), with the Conditional R-squared. The Conditional R-squared is the estimated proportion of variance accounted for by the predictors of the model for each combination of frequency-modality. Significance levels of $p < 00.001$ are reported in ***bold italic***, in *italic* otherwise.

Freq (Hz)	Term	Global				Retinal				Occipital			
		Estimate	P> |z|	OR (95 % CI)	Conditional R-squared	Estimate	P> |z|	OR (95 % CI)	Conditional R-squared	Estimate	P> |z|	OR (95 % CI)	Conditional R-squared
20 Hz	Intercept	***−6.86***	***<0.0001***	***0.00105 (0.000287–0.0033)***	0.7	***−8.36***	***<0.0001***	***0.0002 (0.00003–0.0012)***	0.3	***−5.07***	***<0.0001***	***0.0063 (0.00041–0.009)***	0.05
	dBdt	***1.43***	***<0.0001***	***4.19 (3.51–5.09)***		***1.005***	***<0.0001***	***2.73 (2.15–3.6)***		*0.096*	*0.38*	*1.1 (1.08–1.15)*	
50 Hz	Intercept	***−7.24***	***<0.0001***	***0.0007 (0.0002–0.002)***	0.84	*−7.2*	***<0.0001***	***0.0007 (0.0002–0.0025)***	0.6	***−9.59***	***0.0002***	***0.00007 (0.000000041–0.0037)***	0.45
	dBdt	***0.82***	***<0.0001***	***2.27 (2.06–2.54)***		***0.49***	***<0.0001***	***1.64 (1.52–1.77)***		*0.03*	*0.59*	*1.03 (0.92–1.15)*	
60 Hz	Intercept	***−6.51***	***<0.0001***	***0.0015 (0.0003–0.005)***	0.82	*−10*	***<0.0001***	***0.000043 (0.000044–0.00029)***	0.78	*−7.87*	***<0.0001***	***0.0004 (0.000032–0.0046)***	0.37
	dBdt	***0.61***	***<0.0001***	***1.84 (1.71–2)***		***0.6***	***<0.0001***	***1.82 (1.67–2.01)***		***0.2***	***<0.0001***	***1.23 (1.14–1.31)***	
100 Hz	Intercept	***−7.01***	***<0.0001***	***0.0009 (0.0001–0.004)***	0.56	*−5.97*	***<0.0001***	***0.0025 (0.00041–0.009)***	0.24	***−8.33***	***0.000012***	***0.00024 (0.0000056–0.01)***	0.23
	dBdt	***0.19***	***<0.0001***	***1.21 (1.17–1.26)***		***0.11***	***<0.0001***	***1.11 (1.08–1.15)***		***0.1***	***0.00034***	***1.1 (1.05–1.17)***	

Table 2
The mean 99th percentile *RMS* radial current density (J_n) (i.e., normal to retinal surface) in the retina within 90° and between 90° and 135° from the posterior pole of the eye averaged across 14 head models (± standard deviation). Values were normalized to a *dB/dt* of 1 T/s.

Modality	Segment	$\|J_n\|$ ± sd [(mA/m^2)/(T/s)]	
		Left Eye	Right Eye
GLO	0°–90°	11.01 ± 1.74	10.71 ± 1.95
	90°–135°	12.69 ± 1.21	12.67 ± 1.41
RET	0°–90°	7.90 ± 1.93	6.77 ± 1.41
	90°–135°	11.93 ± 2.01	9.52 ± 1.20
OCC	0°–90°	1.24 ± 0.20	1.13 ± 0.23
	90°–135°	1.47 ± 0.17	1.45 ± 0.22

Table 3
Electrical conductivity of tissues used for dosimetric analysis.

Tissue	Conductivity (S/m)	Tissue	Conductivity (S/m)
Blood	0.7	Glands	0.5
Bone (Cancellous)	0.027	Muscle	0.35
Bone (Cortical)	0.008	Lens	0.32
Brain (Gray matter)	0.2	Scalp	0.4
Brain (White matter)	0.14	Sclera	0.56
Cartilage	0.18	Spinal cord	0.03
Cerebellum	0.2	Tendon	0.3
Cerebrospinal fluid	1.8	Trachea	0.3
Cornea	0.5	Vitreous humor	1.5
Fat	0.08	Retina	0.7

observations hint at a retinal origin for magnetophosphene perception mediated in the rod photoreceptors.

3.1. Dosimetry

To gain a better understanding of the potential underlying substrate in the head involved in the phosphene response, a dosimetric analysis was performed of *B*-field induced current densities (*J*) and *E*-fields, using 14 anatomically accurate 3D-models of the human head. These models featured a realistic geometry and conductivity for each tissue. The scalar values and radial components of the two quantities were calculated with methods similar to those in Nissi and Laakso [23].

Fig. 2 illustrates the distributions of *J* in the head and J_n in the retina for each exposure modality. The right panel shows the induced contours of current flow in the head as dependent on the coils' respective orientations. The left panel displays the distribution of J_n across the retina by modality. The regions with the highest J_n are "crescent-shaped" and are present toward the retina's outer perimeter. For GLO, the regions with maxima occur on the retina's inner and outer lateral surfaces either straddling the equator (90°) for the left and right outer regions and concentrated beyond the equator for the inner regions. RET and OCC display similar patterns of maxima on the retina's caudal surface, with the areas with the highest J_n concentrated beyond the equator.

For the three exposure modalities, the means of the 99th percentile J_n across the 14 head models (± std dev) for inner (0°–90°) and outer (90°–135°) retina are shown in Table 2. For GLO, the 99th percentile J_n is ~15–18 % greater in the outer retina compared to the inner retina, and for RET and OCC ~40–50 % and ~20–30 % greater, respectively. The 50 % response rate thresholds at 20 Hz pooled across Trial were 4.71 T/s for GLO and 7.80 T/s for RET. The corresponding J_n (all values RMS w/std dev) normal to the retinal surface are for GLO with both eyes averaged 51.2 ± 8.7 mA/m^2 for the inner retina and 58.3 ± 6.2 mA/m^2 for outer. For RET, the corresponding J_ns are 61.5 ± 15.1 mA/m^2 (Left eye) and 52.9 ± 11.0 mA/m^2 (Right eye) for the inner retina and 93.1 ± 15.4 mA/m^2 (L) and 74.2 ± 9.1 mA/m^2 (R) for the outer. For OCC, B-

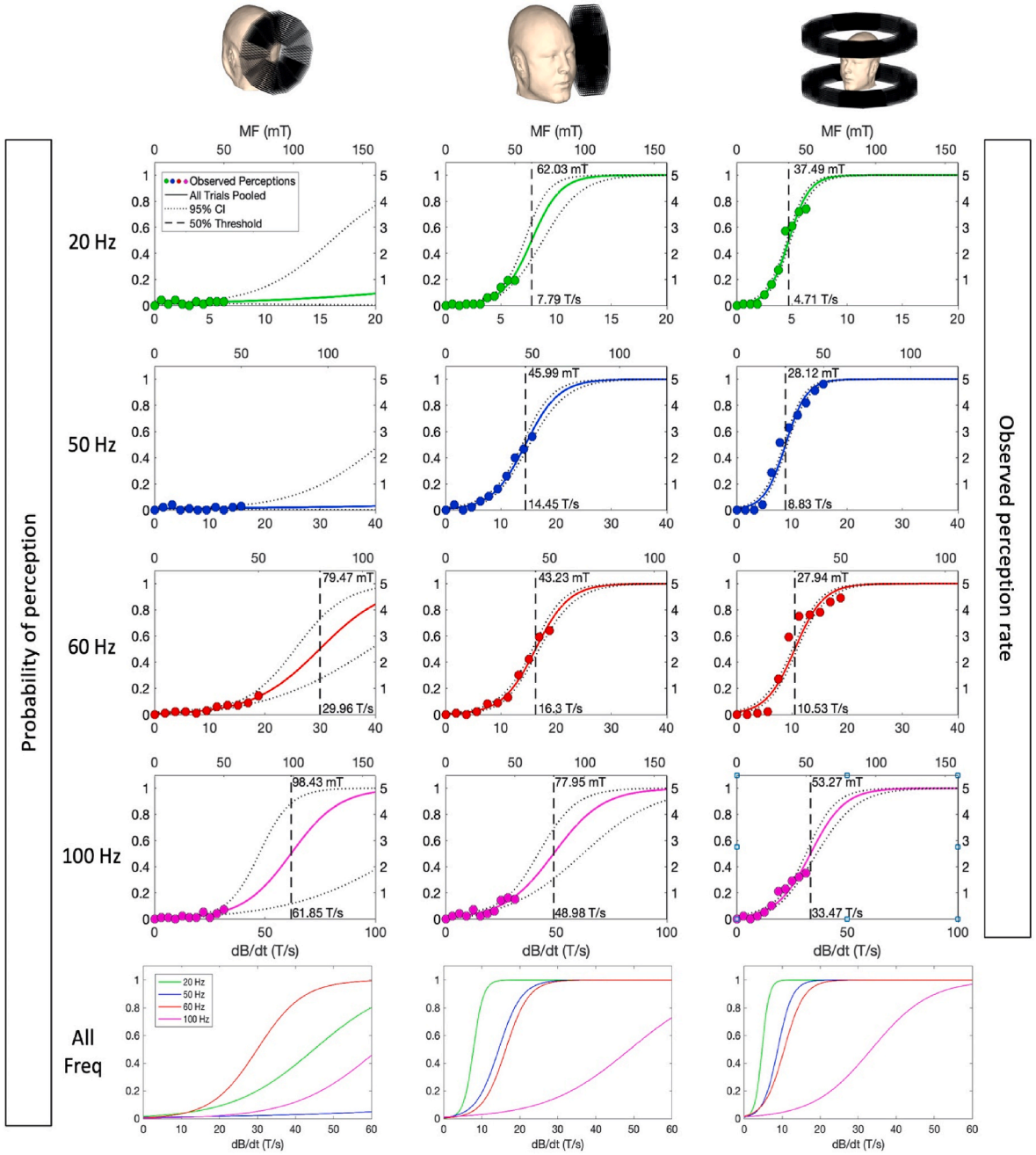

Fig. 1. Top 4 Rows: For each frequency-exposure modality combination, the colored dots represent the mean observed magnetophosphene perception rates vs *dB/dt* (bottom *x*-axes) and *B* (top *x*-axes) pooled across *Trials*. These data points are shown with the logistic regression curves broken out by *Trial* with their collective 95 % *CI*. Bottom Row: The mean magnetophosphene perception curves pooled across *Trials* for each frequency. Vertical axis: probability (or rate) of perception; bottom *x*-axis: *dB/dt* in Tesla per second (T/s); top *x*-axis: *B* in Tesla (T). The field values shown along the bottom (top) *x*-axes indicate *dB/dt* (*B*) corresponding to a 50 % response rate.

fields on the order of 300 mT RMS would be required to induce 50 mA/m^2 RMS, well beyond the exposure system's capabilities.

Since rod cells are located mainly at the retinal periphery and cone cells are mostly absent from this region, the greater J_n in the outer compared to the inner retina at perception threshold is consistent with the participants' report of colorless magnetophosphenes. Furthermore, it suggests that direct modulation of the rod cells is a possible explanation underlying the perception of magnetophosphenes (see Discussion).

4. Discussion

This is the first study linking thresholds of *B*-field-induced phosphenes to anatomically realistic dosimetry of the head (those thresholds being specific to the *B*-fields generated by the exposure system's coils). Our overriding goals were to inform the science of phosphenes, which are commonly induced by tACS experiments, and strengthen the basis for ELF *B*-field health and safety exposure limits. As in previous studies of electro- and magneto-phosphenes [26,4,27,28], response peaked at 20 Hz. The *B*-field exposure-response was statistically significant in all but two conditions (OCC/20 and 50 Hz). The response rate decreased significantly with *Trial* in in the GLO modality at (20 and 50 Hz) and RET

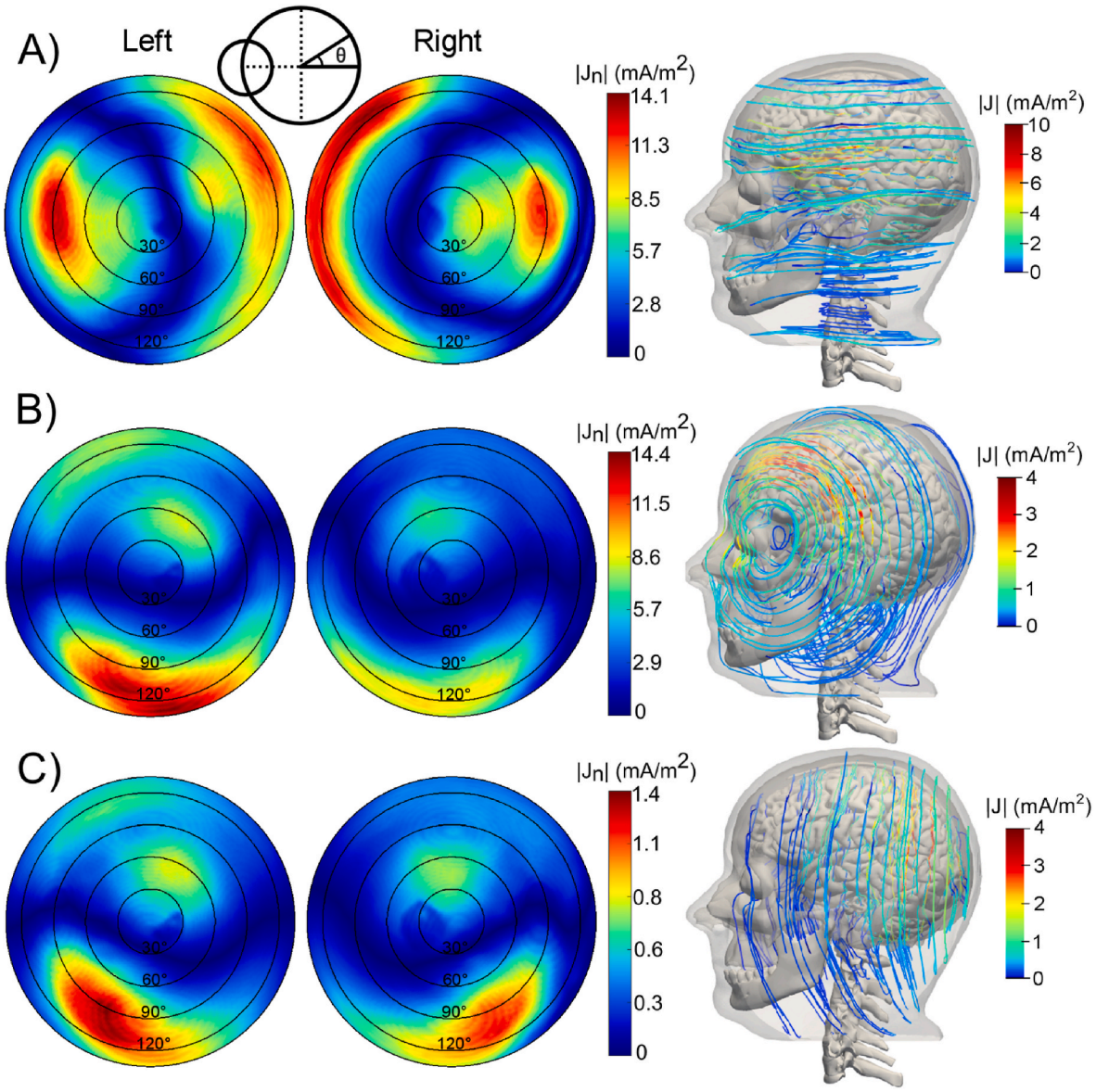

Fig. 2. Anatomically-based dosimetry of induced currents normalized to a *dB/dt* of 1 T/s. On the left are intensities of the current density radial components ($|J_n|$) in the retina viewed from behind (0° at the posterior pole of the eyeball, 90° degrees at the equator, and 135° beyond). On the right are the visualized paths of the induced current within the head. A: Global exposure (GLO). B: Local, retinal exposure (RET). C: Local, occipital exposure (OCC).

(20 and 60 Hz) suggesting adaptation to repeated presentation of the stimulus, darkness, or both. Our objectives were reached with a novel magnetic field exposure system that can achieve tACS-like levels of *in situ* electric field, fully designed in house, powered by MRI amplifiers, featuring water-cooling enabling long exposures (several minutes using continuous sinusoidal fields), and motorized, capable of producing magnetic flux density levels surpassing previous experimental systems (~0.1 T at power-line frequencies), a stimulation modality that we named tAMS. We emphasize that, from a technology perspective, while TMS employs high-amplitude (in the Tesla range) magnetic fields delivered in pulses (less than 1 ms each); tAMS is fundamentally different since it uses sinusoidal magnetic fields of lower intensity. Furthermore, from a neurophysiological perspective, TMS induces *suprathreshold* electric fields in brain tissue, while the electric field induced *in situ* by tAMS is on the order of 1 V/m from our dosimetric analysis (Fig. 3), which is considerably lower than the >100 V/m that are induced with TMS. Therefore, it is unlikely (but not impossible, due to dosimetric uncertainties) that tAMS is able to induce neuronal firing.

Current *B*-field ELF exposure limits are based on small-sample magnetophosphene experiments reported by Lövsund et al. over 40 years ago [4,27], and key results of the earlier studies with ours are shown in Supp. Table 1 and Supp. Fig. 2, respectively. Our study attempted to improve several aspects of these earlier studies, especially those from the Lövsund studies, as highlighted in the Supp. Table 1 (e.g., field heterogeneity to homogeneity, small n-sizes to bigger groups, improved method for phosphenes perception, frequencies tested, various to consistent light conditions). Here, by avoiding biases (e.g., switching transients) present in this older data, we provide data that is key both in terms of tACS mechanistic understanding and EMF exposure guidelines. From the tACS perspective, we provide evidence for, while not being definitive proof of, phosphene generation resulting exclusively through interaction with the retina, favoring this hypothesis as compared to a direct stimulation of occipital cortex neurons. In terms of direct contribution to EMF exposure guidelines, this supports that the required electric field to generate magnetophosphene is higher than previously thought, indicating that the current threshold limit is too conservative (i.e., unnecessarily high), and thereby confirmed to be safe. Indeed, we provide the first data on magnetophosphene thresholds due

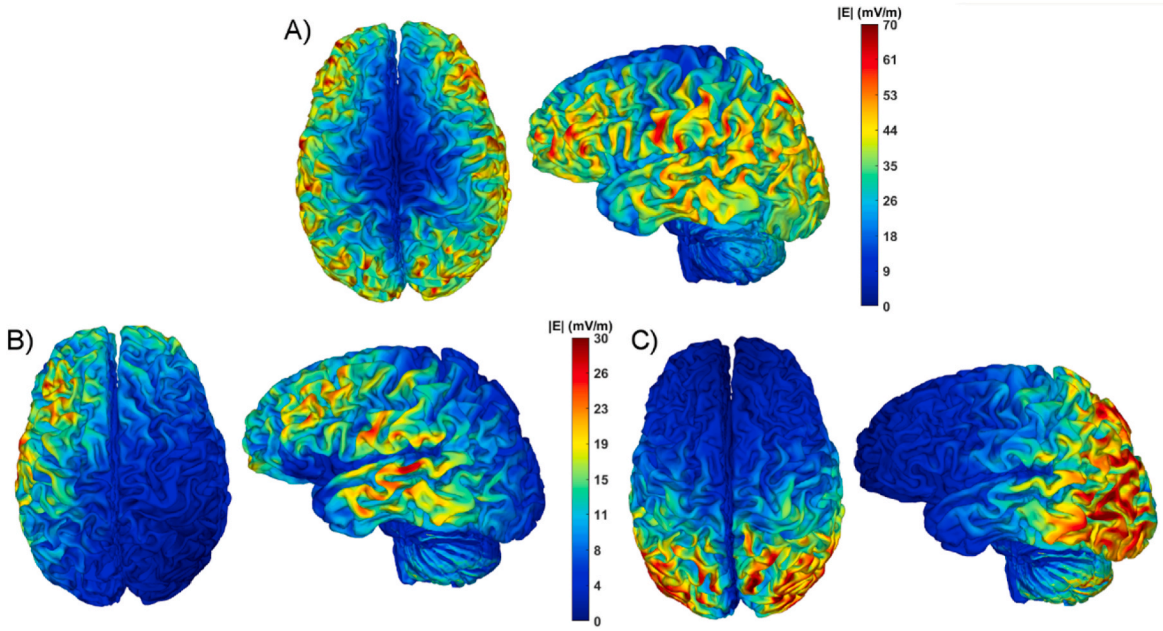

Fig. 3. Anatomic dosimetry of induced electric fields in the cortex normalized to a dB/dt of 1 T/s. The induced E-field was also determined on the surface of the cortex at a depth of 2 mm. A: Global exposure. B: Retinal exposure. C: Occipital exposure.

exposure to a uniform magnetic field at utility frequencies. Currently, the exposure limits to, e.g., magnetic fields emitted from electrical appliances and industrial applications, have been derived directly by applying reduction/safety factors to estimated magnetophosphene thresholds [13,14], extrapolating 10–45 Hz localized exposure data to uniform fields at 50 and 60 Hz. We also provide new data on the induced dosimetric quantities corresponding to the measured phosphene thresholds, which can be directly relevant for the development of exposure limits, which are given in terms of *in situ* electric field values estimated using simplified models [28].

A lingering question is whether neural input from the occipital cortex alone produces a phosphene response. Transcranial alternating current stimulation (tACS) experiments with alpha- and beta band (8–30 Hz) currents applied into various sites, including the occipital cortex [11,13,17,29,30], have documented phosphene responses, with some suggestions [11,13,17] (but not concrete evidence) of a direct effect. Laakso and Hirata demonstrated that tACS current from the scalp through the retina can exceed the phosphene threshold [19]. If the phosphene responses originate from the retina, we would expect that the threshold in terms of dB/dt for the RET condition would be on average 40–50 % higher than that for the GLO modality, given that the current density values for the same dB/dt are lower for RET than for GLO (0°–90° segment in Table 2). The measured dB/dt thresholds (Fig. 1) for the GLO and RET modalities agreed with this estimated relationship. Similarly, the dB/dt threshold for the OCC modality should be on average 6–9 times that for the RET or GLO modalities, which would require magnetic flux densities exceeding the maximum of 50 mT $_{RMS}$ used in the measurements. Consistently with this prediction, the phosphene thresholds could not be determined for the OCC modality, even though the coil system delivered *E*-fields to the occipital cortex (Fig. 3) equivalent to the *E*-fields delivered by tACS [31]. Thus, our data does not substantiate phosphenes as originating from the visual cortex alone without retinal contribution. Furthermore, given the levels of *in situ* electric field in the occipital cortex from 50 mT *RMS* (<1 V/m), and the small polarizability of neuron membranes by electric fields (on the order of 0.2 mV per V/m of applied electric field, as reviewed in Modolo et al. [32]), it is physiologically implausible for occipital cortex neurons to trigger action potentials from the OCC modality.

In terms of biophysical mechanisms of magnetophosphene perception, dosimetry together with the subjects' reports of phosphenes in their peripheral visual field (Table 2) strongly suggest rod cells, - concentrated in the retina's periphery - as the sensory transducer. As reflected in Fig. 2 and Table 2, current density doses to the retina in its 90°–135° segment were greater compared to the 0°–90° segment (17 % for GLO; 40–50 % for RET), an observation that is consistent with - but does not prove - rod involvement. Also, with maximum sensory response at 20 Hz, magnetophosphene perception is in line with the frequency sensitivity of rods [33]. Further, rod signaling is graded, as opposed to all-or-none, thus encoding small changes in membrane potential, and an action potential is not required for downstream neuromodulatory effects (e.g., in bipolar cells). Also, Lövsund et al. reported the magnetophosphene threshold increasing with time during dark adaptation [4], and Schwarz (as displayed in Schwiedrzik, 2009 [34]) observed the effect with electrophosphenes.

5. Conclusion

Our results expand the understanding of electric and magnetic stimulus interactions with the visual system, and also inform health and safety standard development. The basic and applied aspects of the study benefited from the "marriage" of the response behavior with modality-specific dosimetry. Although current evidence in the tACS literature does not rule out the possible contribution of occipital cortex-to-eye neural pathways, our data support generation of phosphenes locally. Uncertainty remains with respect to the specific loci of interactions within the retina. Further, a ready explanation for the positive responses observed at 60 and 100 Hz for OCC exposure remains unknown, but the responses were very weak relative to GLO and RET, and false positives due to any number of possible unrelated factors cannot be automatically ruled out.

Finally, it is important to highlight once again the unique technical innovations that enabled this study. Indeed, the MF exposure system developed for these experiments was able to induce of E-fields similar in intensities to those produced by tACS, but without contact with the head, and without well-known tACS limitations, which include skin sensations beneath the stimulation electrodes, the difficulty to cope with the skin and bone and current shunting. These overall, and as pointed as by some previous works, these effects cloud the ability to discriminate

the effects of injected currents from peripheral sensory effects. We argue that MF induction overcomes such difficulties and should be considered as an alternative to tACS.

CRediT authorship contribution statement

Alexandre Legros: Writing – review & editing, Writing – original draft, Visualization, Validation, Supervision, Resources, Project administration, Methodology, Investigation, Funding acquisition, Formal analysis, Data curation, Conceptualization. **Janita Nissi:** Writing – review & editing, Writing – original draft, Visualization, Software, Resources, Methodology. **Ilkka Laakso:** Writing – review & editing, Writing – original draft, Visualization, Validation, Supervision, Software, Resources, Methodology, Investigation. **Joan Duprez:** Data curation, Formal analysis. **Robert Kavet:** Writing – review & editing, Writing – original draft, Methodology, Formal analysis, Data curation. **Julien Modolo:** Writing – review & editing, Writing – original draft, Validation, Software, Resources, Methodology, Investigation, Formal analysis, Conceptualization.

Declaration of competing interest

On the behalf of all the co-authors, I declare that neither me nor the co-authors have no known competing financial interests or personal relationships that could have appeared to influence the work reported in this paper.

Acknowledgments

This project was sponsored by: Hydro-Québec (Canada) (http://www.hydroquebec.com/en/); EDF-RTE (France) (http://www.edf.com/the-edf-group-42667.html) (http://www.rte-france.com/fr/); CIHR (Canada, grant #187204) (http://www.cihr-irsc.gc.ca/e/193.html); CFI/ORF (Canada, Biomedical Multimodality Hybrid Imaging – grant #11358) (http://www.innovation.ca/en); and the Lawson Health Research Institute (http://www.lawsonresearch.com). The funders had no role in study design, data collection and analysis, decision to publish, or preparation of the manuscript. The authors also wish to acknowledge Mr. Lynn Keenliside for his instrumental contribution to designing and building the exposure systems, and Dr. Joan Duprez for his contribution to the statistical analysis.

Appendix A. Supplementary data

Supplementary data to this article can be found online at https://doi.org/10.1016/j.brs.2024.05.004.

References

[1] D'Arsonval A. Dispostifis pour la mesure des courants alternatifs de toutes frequences. Comput. Rendus. Soc. Biol. 1896;450–451.
[2] Lövsund P, Öberg PÅ, Nilsson SEG. Magnetophosphenes: a quantitative analysis of thresholds. Med Biol Eng Comput 1980;18:326–34.
[3] Barlow H, Kohn H, Walsh E. The effect of dark adaptation and of light upon the electric threshold of the human eye. Am J Physiol 1947;148:376–81.
[4] Lovsund P, Oberg PA, Nilsson SE. Influence on vision of extremely low frequence electromagnetic fields. Industrial measurements, magnetophosphene studies volunteers and intraretinal studies in animals. Acta Ophthalmol 1979;57:812–21.
[5] Brindley GS. The site of electrical excitation of the human eye. J Physiol 1955;127:189–200.
[6] Potts A, Inoue J. The electrically evoked response of the visual system (EER). 3. Further contribution to the origin of the EER. Invest Ophthalmol 1970;9:814–9.
[7] Knighton RW. An electrically evoked slow potential of the frog's retina. I. Properties of response. J Neurophysiol 1975;38:185–97.
[8] Evans ID, Palmisano S, Loughran SP, Legros A, Croft RJ. Frequency-dependent and montage-based differences in phosphene perception thresholds via transcranial alternating current stimulation. Bioelectromagnetics 2019;40.
[9] Institute of Electrical and Electronics Engineers (IEEE). IEEE standard for safety levels with respect to human exposure to electric, magnetic, and electromagnetic fields, 0 Hz to 300 GHz. IEEE Std C95.1-2019 2019. Preprint at.
[10] ICNIRP. Guidelines for limiting exposure to time-varying electric and magnetic fields (1 Hz to 100 kHz). Health Phys 2010;99:818–36.
[11] Kanai R, Chaieb L, Antal A, Walsh V, Paulus W. Frequency-dependent electrical stimulation of the visual cortex. Curr Biol 2008;18:1839–43.
[12] Kar K, Krekelberg B. Transcranial electrical stimulation over visual cortex evokes phosphenes with a retinal origin. J Neurophysiol 2012;108:2173–8.
[13] Evans ID, Palmisano S, Loughran SP, Legros A, Croft RJ. Frequency-dependent and montage-based differences in phosphene perception thresholds via transcranial alternating current stimulation. Bioelectromagnetics 2019;40.
[14] Naycheva L, et al. Phosphene thresholds elicited by transcorneal electrical stimulation in healthy subjects and patients with retinal diseases. Invest Ophthalmol Vis Sci 2012;53:7440–8.
[15] Kavet R, Bailey WH, Bracken TD, Patterson RM. Recent advances in research relevant to electric and magnetic field exposure guidelines. Bioelectromagnetics 2008;29:499–526.
[16] Saunders RD, Jefferys JG. A neurobiological basis for ELF guidelines. Health Phys 2007;92:596–603.
[17] Evans ID, Palmisano S, Croft RJ. Retinal and cortical contributions to phosphenes during transcranial electrical current stimulation. Bioelectromagnetics 2021;42:146–58.
[18] Laakso I, Hirata A. Computational analysis shows why transcranial alternating current stimulation induces retinal phosphenes. J Neural Eng 2013;10:046009.
[19] Laakso I, Hirata A. Computational analysis of thresholds for magnetophosphenes. Phys Med Biol 2012;57:6147–65.
[20] Bates D, Mächler M, Bolker BM, Walker SC. Fitting linear mixed-effects models using lme4. J Stat Software 2015;67.
[21] lme4 citation info. https://cran.r-project.org/web/packages/lme4/citation.html.
[22] R Core Team. R A language and environment for statistical computing. Vienna. - References - Scientific Research Publishing: R Foundation for Statistical Computing; 2023. https://www.scirp.org/reference/referencespapers?referenceid=3582659.
[23] Nissi J, Laakso I. Magneto- and electrophosphene thresholds in the retina: a dosimetry modeling study. Phys Med Biol 2022;67:015001.
[24] Soldati M, Laakso I. Computational errors of the induced electric field in voxelized and tetrahedral anatomical head models exposed to spatially uniform and localized magnetic fields. Phys Med Biol 2020;65.
[25] Nissi J, Laakso I. Magneto- and electrophosphene thresholds in the retina: a dosimetry modeling study. Phys Med Biol 2022;67:015001.
[26] Gebhard JW. Thresholds of the human eye for electric stimulation by different wave forms. J Exp Psychol 1952;44:132–40.
[27] Lövsund P, Öberg PÅ, Nilsson SEG, Reuter T. Magnetophosphenes: a quantitative analysis of thresholds. Med Biol Eng Comput 1980;18:326–34.
[28] Marg E, Rudiak D. Phosphenes induced by magnetic stimulation over the occipital brain: description and probable site of stimulation. Optom Vis Sci 1994;71:301–11.
[29] Evans I, Palmisano S, Croft RJ. Effect of ambient lighting on frequency dependence in transcranial electrical stimulation-induced phosphenes. Sci Rep 2022;12:1–9. 2022 12.
[30] Kar K, Krekelberg B. Transcranial electrical stimulation over visual cortex evokes phosphenes with a retinal origin. J Neurophysiol 2012;108:2173–8.
[31] Herrmann CS, Rach S, Neuling T, Strüber D. Transcranial alternating current stimulation: a review of the underlying mechanisms and modulation of cognitive processes. Front Hum Neurosci 2013;7.
[32] Modolo J, Denoyer Y, Wendling F, Benquet P. Physiological effects of low-magnitude electric fields on brain activity: advances from in vitro, in vivo and in silico models. Curr Opin Biomed Eng 2018;8:38–44.
[33] Verweij J, Dacey DM, Peterson BB, Buck SL. Sensitivity and dynamics of rod signals in H1 horizontal cells of the macaque monkey retina. Vis Res 1999;39:3662–72.
[34] Schwiedrzik CM. Retina or visual cortex? The site of phosphene induction by transcranial alternating current stimulation. Front Integr Neurosci 2009;3:1839–43.